Available online at www.sciencedirect.com
SCIENCE DIRECT®
Control Engineering Practice 13 (2005) 699–711
CONTROL ENGINEERING PRACTICE
www.elsevier.com/locate/conengprac

Reconfigurable control structure to prevent the rollover of heavy vehicles ☆

P. Gaspar[a,*], I. Szaszi[b], J. Bokor[a]

[a] *Computer and Automation Research Institute, Hungarian Academy of Sciences, Systems and Control Laboratory, Kende u. 13-17, 1111 Budapest, Hungary*

[b] *Department of Control and Transport Automation, Budapest University of Technology and Economics, Budapest, Hungary*

Received 16 May 2003; accepted 4 June 2004
Available online 30 July 2004

Abstract

In this paper a reconfigurable control structure is developed to reduce the risk of heavy vehicles rolling over. The control structure with an active anti-roll bar control and an active brake control is combined with a fault detection and identification (FDI) filter, which identifies different actuator failures. The control design uses the linear parameter varying model of the vehicle, in which the forward velocity, the lateral load transfer and the residual output of the FDI filter are selected as scheduling parameters. The design of the FDI filter is based on the $\mathscr{H}_\infty$ filtering method. The operation of the reconfigurable control mechanism are demonstrated in various vehicle manoeuvres.

Keywords: Vehicle dynamics; Nonlinear control systems; Active control; Robustness; Linear parameter varying control

1. Introduction and motivation

The aim of preventing rollovers is to provide the vehicle with an ability to resist overturning moments generated during cornering. Several schemes with possible active intervention into the vehicle dynamics have been proposed. One of these methods employs active anti-roll bars, that is, a pair of hydraulic actuators which generate a stabilizing moment to balance the overturning moment (see Abe, 1994; Lin, Cebon, & Cole, 1996; Sampson & Cebon, 1998). Another method applies active steering since it affects lateral acceleration directly (see Ackermann, Odenthal, & Bunte, 1999; Ackermann & Odenthal, 1999). The third method applies an electronic brake mechanism to reduce the lateral tire forces acting on the outside wheel (see Chen & Peng, 2001; Frank, Palkovics, & Gianone, 2000; Palkovics, Semsey, & Gerum, 1999).

The disadvantage of the active anti-roll bars is that the maximum stabilizing moment is limited physically by the relative roll angle between the body and the axle. In the case of active steering as well as brake control the only physical limit is the actuator saturation. These compensators, however, have effects on not only the roll dynamics of the vehicle but they also modify the desired path of the vehicle, so they affect the yaw motion. The different control structures should be combined in one control mechanism, e.g. the linear steering control is supplemented with nonlinear emergency steering and brake control (see Odenthal, Bunte, & Ackermann, 1999). The success of these solutions requires the faultless operation of the control mechanism. Fault detection and identification (FDI) are important in the yaw-roll dynamics since the stability of the vehicle is degraded by different faults.

Significant research results have been published on the general FDI problem (see Gertler, 1997; Massoumnia, 1986; Szigeti, Vera, Bokor, & Edelmayer, 2001). The

☆This project has been supported by the Hungarian National Science Foundation under grant number T-030182, which is gratefully acknowledged.

*Corresponding author. Tel.: +36-127-961-71; fax: +36-146-675-03.

E-mail address: gaspar@sztaki.hu (P. Gaspar).

0967-0661/$ - see front matter © 2004 Elsevier Ltd. All rights reserved.
doi:10.1016/j.conengprac.2004.06.003

design of FDI filters in the field of vehicle industry has been proposed in several papers (see e.g. Isermann, 2001; Jeppesen & Cebon, 2001). There are also numerous papers dealing with the design of reconfigurable controls, which include the design of the FDI filter, the design of the reconfigurable controller and the design of the reconfiguration mechanism. Applications of the reconfigurable control systems can be found in different fields (see e.g. Szaszi, Marcos, Balas, & Bokor, 2001; Ganguli, Marcos, Balas, & Bokor, 2002; Isermann, Schwarz, & Stolz, 2002; Kanev & Verhaegen, 2000).

In our project a combined control mechanism, in which both the active anti-roll bars and the active brake control are applied, has been developed. This control structure also results in a fault-tolerant system since in case of a failure an adequate tuning of the control mechanism guarantees the roll stability. The control design is based on an linear parameter varying (LPV) model, in which the forward velocity of the vehicle, the normalized lateral load transfer and the residual output of the FDI filter are applied as scheduling parameters in order to focus on performance specifications. This method applies the Lyapunov quadratic stability criterion with respect to uncertainties. In the combined control the fault information is an input signal, which is generated by the FDI filter.

The purpose of the FDI filter is to identify the different actuator failures together with the time of their occurrence and their values. The FDI filter design is based on the LPV model of the vehicle, in which the scheduling parameter is the forward velocity of the vehicle. In the case of a detected failure the operation of the control mechanism must be modified. For this purpose, the normalized fault parameter is also applied as a scheduling parameter. Using fault information this reconfigurable feature leads to an enhanced roll stability when a fault occurs in the hydraulic actuator.

The paper is organized as follows. In Section 2 a combined control mechanism with the active anti-roll bars and the active brake is discussed. In Section 3 the reconfigurable control is designed by applying an LPV FDI filter. In Section 4 the FDI filter is tested during various vehicle maneuvers. Section 5 contains some concluding remarks.

2. The combined control of vehicle dynamics to prevent rollovers

Fig. 1 illustrates the combined yaw-roll dynamics of the vehicle modelled by a three-body system, in which m_s is the sprung mass, $m_{u,f}$ is the unsprung mass at the front including the front wheels and axle, and $m_{u,r}$ is the unsprung mass at the rear with the rear wheels and axle. In the vehicle modelling the motion differential equations of the yaw-roll dynamics of the single unit vehicle, i.e. the lateral dynamics, the yaw moment, the roll moment of the sprung mass, the roll moment of the front and the rear unsprung masses, are formalized.

$$mv(\dot{\beta}+\dot{\psi}) - m_s h\ddot{\phi} = F_{y,f} + F_{y,r}, \tag{1}$$

$$-I_{xz}\ddot{\phi} + I_{zz}\ddot{\psi} = F_{y,f}l_f - F_{y,r}l_r + l_w\Delta F_b, \tag{2}$$

$$\begin{aligned}(I_{xx}+m_s h^2)\ddot{\phi} - I_{xz}\ddot{\psi} &= m_s g h\phi + m_s v h(\dot{\beta}+\dot{\psi}) \\ &\quad - k_f(\phi-\phi_{t,f}) - b_f(\dot{\phi}-\dot{\phi}_{t,f}) + u_f \\ &\quad - k_r(\phi-\phi_{t,r}) - b_r(\dot{\phi}-\dot{\phi}_{t,r}) + u_r,\end{aligned} \tag{3}$$

$$\begin{aligned}-h_r F_{y,f} &= m_{u,f} v(h_r - h_{u,f})(\dot{\beta}+\dot{\psi}) + m_{u,f} g h_{u,f}\phi_{t,f} \\ &\quad - k_{t,f}\phi_{t,f} + k_f(\phi-\phi_{t,f}) \\ &\quad + b_f(\dot{\phi}-\dot{\phi}_{t,f}) + u_f,\end{aligned} \tag{4}$$

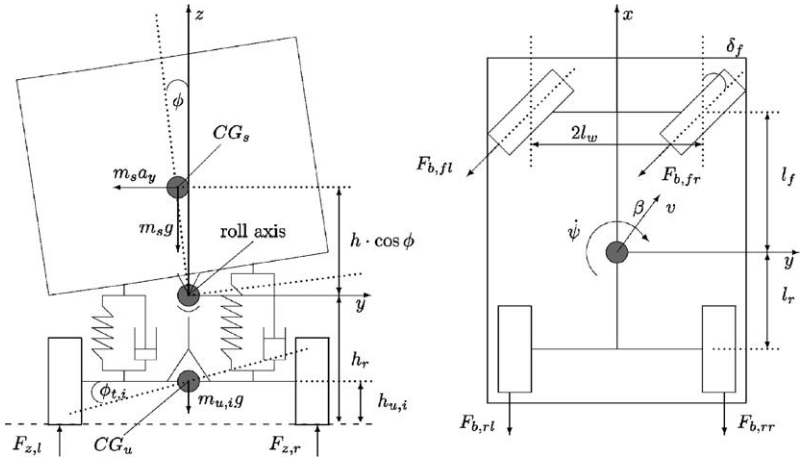

Fig. 1. Rollover vehicle model.

Table 1
Symbols of the yaw-roll model

Symbols	Description
m_s	sprung mass
$m_{u,i}$	unsprung mass
m	the total vehicle mass
v	forward velocity
v_{wi}	components of the forward velocity
h	height of CG of sprung mass from roll axis
$h_{u,i}$	height of CG of unsprung mass from ground
h_r	height of roll axis from ground
a_y	lateral acceleration
β	side-slip angle at center of mass
ψ	heading angle
$\dot{\psi}$	yaw rate
α	side slip angle
ϕ	sprung mass roll angle
$\phi_{t,i}$	unsprung mass roll angle
δ_f	steering angle
u_i	control torque
ΔF_b	difference between the braking forces
C_i	tire cornering stiffness
$F_{y,i}$	lateral tire force
F_{zi}	total axle load
$\Delta F_{z,i}$	lateral load transfer
R_i	normalized load transfer
k_i	suspension roll stiffness
b_i	suspension roll damping
$k_{t,i}$	tire roll stiffness
I_{xx}	roll moment of inertia of sprung mass
I_{xz}	yaw-roll product of inertial of sprung mass
I_{zz}	yaw moment of inertia of sprung mass
l_i	length of the axle from the CG
l_w	half of the vehicle width
μ	road adhesion coefficient

$$-h_r F_{y,r} = m_{u,r} v(h_r - h_{u,r})(\dot{\beta} + \dot{\psi}) - m_{u,r} g h_{u,r} \phi_{t,r} - k_{t,r}\phi_{t,r} + k_r(\phi - \phi_{t,r}) + b_r(\dot{\phi} - \dot{\phi}_{t,r}) + u_r. \quad (5)$$

The detailed derivation of the equations of the yaw-roll dynamics of the single unit vehicle can be found in Sampson and Cebon (2003). The symbols of the yaw-roll model are found in Table 1.

The lateral tire forces $F_{y,i}$ in the direction of velocity at the wheel ground contact points are approximated proportionally to the tire side slip angle α_i.

$$F_{y,f} = \mu C_f \alpha_f, \quad (6a)$$

$$F_{y,r} = \mu C_r \alpha_r. \quad (6b)$$

The C_i is the tire side slip constant and α_i is the tire side slip angle associated with the front and rear axles. The chassis and the wheels have identical velocities at the wheel ground contact points. The velocity equations for the front and rear wheels in the lateral and in the longitudinal directions are as follows:

$$v_{w,f}\sin(\delta_f - \alpha_f) = l_f \cdot \dot{\psi} + v\sin\beta, \quad (7a)$$

$$v_{w,f}\cos(\delta_f - \alpha_f) = v\cos\beta, \quad (7b)$$

$$v_{w,r}\sin\alpha_r = l_r \cdot \dot{\psi} - v\sin\beta, \quad (7c)$$

$$v_{w,r}\cos\alpha_r = v\cos\beta. \quad (7d)$$

In stable driving conditions, the tire side slip angle α_i is normally not larger than 5° and the above equation can be simplified by substituting $\sin x \approx x$ and $\cos x \approx 1$. The classic equations for the tire side slip angles are then given as

$$\alpha_f = -\beta + \delta_f - \frac{l_f \cdot \dot{\psi}}{v}, \quad (8a)$$

$$\alpha_r = -\beta + \frac{l_r \cdot \dot{\psi}}{v}. \quad (8b)$$

The Eqs. (1)–(5) can be expressed in the state space representation form. The system states are the side slip angle of the sprung mass β, the yaw rate $\dot{\psi}$, the roll angle ϕ, the roll rate $\dot{\phi}$, the roll angle of the unsprung mass at the front axle $\phi_{t,f}$ and at the rear axle $\phi_{t,r}$. Let the state vector be the following:

$$x = [\beta\ \dot{\psi}\ \phi\ \dot{\phi}\ \phi_{t,f}\ \phi_{t,r}]^{\mathrm{T}}. \quad (9)$$

Using the state vector, the differential algebraic model defined by Eqs. (1)–(5) is transformed into a state space representation form:

$$E(v)\dot{x} = A_0(v)x + B_{01}\delta_f + B_{021}u_c + B_{022}\Delta F_b, \quad (10)$$

where $E(v)$, which contains masses and inertias, is an invertible matrix. Multiplying the left and right-hand side of this equation by the $E^{-1}(v)$, the state space representation is yielded:

$$\dot{x} = A(v)x + B_1(v)\delta_f + B_{21}(v)u_c + B_{22}(v)\Delta F_b, \quad (11)$$

where δ_f is the front wheel steering angle. The control inputs are the roll moments between the sprung and unsprung masses generated by the active anti-roll bars, $u_c = [u_f\ u_r]$, and the difference in brake forces between the left and right-hand sides of the vehicle, ΔF_b.

In the paper it is assumed that the difference in the brake forces ΔF_b provided by the compensator is applied on the rear axle. This means that only one wheel is decelerated at the rear axle. This deceleration generates an appropriate yaw moment. This assumption does not restrict the implementation of the compensator because it is possible that the control action be distributed at the front and the rear wheels on either side. In this case a sharing logic is required, which calculates the brake forces for the wheels.

In the Eq. (11) the matrices depend on the forward velocity of the vehicle nonlinearly. In the linear yaw-roll model the forward velocity is considered a constant

Table 2
Parameters of the yaw-roll model

Parameters	Value
m_s	12 487 kg
m_{uf}, m_{ur}	706 kg, 1000 kg
m	14 193 kg
h_r	1.15 m
$h_{uf} h_{ur}$	0.53 m, 0.53 m
r	0.83 m
C_f, C_r	582×10^3 kN/rad, 783×10^3 kN/rad
k_f, k_r	380×10^3 kN m/rad, 684×10^3 kN m/rad
b_f, b_r	100×10^3 kN/rad, 100×10^3 kN/rad
$k_{t,f}, k_{t,f}$	2060×10^3 kN m/rad, 3337×10^3 kN m/rad
I_{xx}	24 201 kg m^2
I_{xz}	4200 kg m^2
I_{zz}	34 917 kg m^2
l_f, l_r	1.95 m, 1.54 m
l_w	0.93 m
μ	1

parameter (Table 2). However, the forward velocity is an important stability parameter, so that it is considered to be a variable of the motion. The forward velocity is approximately equivalent to the velocity in the longitudinal direction while the side slip angle β is small. It can be assumed that the side slip angle is small under stable driving conditions. Hence the driving throttle is constant during a lateral maneuver and the forward velocity only depends on the brake forces.

The class of finite dimensional linear systems, whose state space entries depend continuously on a time varying parameter vector, $\rho(t)$, is called LPV. The trajectory of the vector-valued signal, $\rho(t)$ is assumed not to be known in advance, although its value is accessible (measured) in real time and is constrained a priori to lie in a specified bounded set. The idea behind using LPV systems is to take advantage of the casual knowledge of the dynamics of the system (see Becker & Packard, 1994; Leith & Leithead, 2000; Rough & Shamma, 2000; Wu, 2001). The formal definition of an LPV system is given below:

Definition 1. For a compact subset $\mathscr{P} \subset \mathscr{R}^S$, the parameter variation set $\mathscr{F}_{\mathscr{P}}$ denotes the set of all piecewise continuous functions mapping $\mathscr{R}$ (time) into $\mathscr{P}$ with a finite number of discontinuities in any interval. The compact set $\mathscr{P} \subset \mathscr{R}^S$, along with continuous functions $A : \mathscr{R}^S \to \mathscr{R}^{n \times n}$, $B : \mathscr{R}^S \to \mathscr{R}^{n \times n_u}$ represents an nth order LPV system $G(\rho)$ whose dynamics evolve as

$$\dot{x} = A(\rho)x + B(\rho)u, \tag{12}$$

where $\rho \in \mathscr{F}_{\mathscr{P}}$.

One characteristics of the LPV system is that it must be linear in the pair formed by the state vector, x, and the control input vector, u. The matrices A and B are generally nonlinear functions of the scheduling vector ρ. In our case the state space representation dependence on velocity is nonlinear (see Eq. (11)). Choosing the forward velocity v as a scheduling parameter, the differential equations of the yaw-roll motion are linear in the state variables: $\rho = v$.

The objective of the combined roll stability control system is to use both the roll moment from the active anti-roll bars and the controlled brake system to maximize the roll stability of the vehicle. The rollover is caused by the high lateral inertial force generated by lateral acceleration. If the position of the center of gravity is high or the forward velocity of the vehicle is larger than allowed at a given steering angle the resulting lateral acceleration is also large and might initiate a rollover. An imminent rollover can be detected if the normalized lateral load transfer is calculated in the following way:

$$R_i = \frac{\Delta F_{z,i}}{F_{z,i}}, \tag{13}$$

where $\Delta F_{z,i} = k_{t,i}\phi_{t,i}/l_w$ is the lateral load transfer for the axles and $F_{z,i}$ is the total axle load. By varying the control torques between the sprung and unsprung masses the active roll control system can manipulate the axle load transfers and the body-roll angles. Moreover using the brake system of the vehicle a yaw moment can be generated by unilateral brake forces, which can reduce the lateral acceleration directly.

The goal is to design a controller that uses the active anti-roll bars all the time to prevent the rollover and activates the controlled braking system only when the vehicle comes close to the rolling over. In a normal driving situation the brake part of the controller should not be activated. However if the normalized load transfer reaches a critical value the brake system must minimize the lateral acceleration to prevent the rollover. The critical value of the normalized load transfer is determined when the load transfer of one of the curve-inner wheels tends to zero.

3. Reconfigurable control to improve fault-tolerant behavior

One possible extension of the combined control strategy proposed here is to design a fault-adaptive rollover control system. In a non-faulty case both the active anti-roll bars and the brake system operate well. The brake system is only active when the normalized load transfer has reached its critical value R_{crt}. In a non-faulty case, it would be preferable to choose R_{crt} large. This corresponds to an active brake system that is not used for most of the time, but which is activated very rapidly as the normalized load transfer exceeds the

critical value determined by R_{crt}. In this case it is assumed that the controlled brake system is used in an emergency most of the time. Although this would result in a large lateral acceleration until the critical R_{crt} has been reached. This would be a small price to pay for the stability of yaw motion. Because until the critical R_{crt} is reached only the active anti-roll bars are used, which do not affect the yaw dynamics of the vehicle. On the other hand, if a hydraulic actuator fault occurs in the system, it would be preferable to choose the critical value of normalized load transfer R_{crt} small. In other words it means that the range of operation of the brake system is extended and the wheels are decelerated gradually rather than rapidly if the normalized load transfer reaches its critical value. It is assumed that the actuator fault can occur in such a way, e.g. where it loses its effectiveness, i.e. its performance is reduced. It means that both control inputs (the active anti-roll bars and the brake system) are able to work simultaneously but the hydraulic actuator does not have maximum performance. It is a reasonable assumption in many cases because the occurrence of a failure causes an effectiveness failure at an early stage. Thus, the R_{crt} can be regarded as a design parameter in the control design, hence it should be chosen to be scheduled on fault information. The fault information is provided by an FDI filter. This adaptive feature would lead to enhanced roll stability using fault information when a fault occurs in the hydraulic actuators.

3.1. Fault detection for actuator failures

Several methods have been proposed for the general FDI problem, e.g. the parity space approach, the multiple model method, the detection filter design using a geometric approach, or the dynamic inversion based detection (see Gertler, 1997; Massoumnia, 1986; Szigeti et al., 2001). Most of the design approaches refer to linear, time-invariant (LTI) systems, but references to some nonlinear cases can also be found in the literature (see Hammouri, Kinnaert, & Yaagoubi, 1999; Chen & Patton, 1999; Stoustrup & Niemannn, 1998; Persis & Isidori, 2001). The geometric approach to the design of detection filters was initiated by Massoumnia (1986) for LTI systems and was also used by Edelmayer, Bokor, Szigeti, and Keviczky (1997) for linear time varying (LTV) systems, and (Bokor & Balas, 2004; Szabo, Bokor, & Balas, 2002) for LPV systems. An $\mathscr{H}_\infty$ approach to the design of an FDI gain scheduled filter for polytopic LPV systems was presented by Abdalla, Nobrega, and Grigoriadis (2001). Another method transforms the nonlinear system into an upper linear fractional transformation (LFT) form, which is the basis of the FDI design (see Stoustrup & Niemannn, 1998). A complete analysis of the combined feedback controller and fault detection filter for both nominal and uncertain systems has been carried out (see Niemann & Stoustrup, 1997a,b).

In order to enhance the fault tolerant behavior of the roll stability system actuator fault information provided by the FDI filter must be used. In this section the LPV FDI filter design is considered. The design of the FDI filter is based on the LPV model of the vehicle, in which the scheduling parameter is the forward velocity. The design of the controller is independent from the design of the FDI filter. The goal is to design an FDI filter which can detect the failures in both the actuators occurring at the front and rear active anti-roll bars. If either of the actuators fails then the control algorithm must be reconfigured, that is the operation regime of the brake system must be extended.

Consider the weighted open-loop system in Fig. 2, which includes the LPV yaw-roll model, the parameter dependent FDI filter, and elements associated with performance objectives. The scheduling parameter is the forward velocity: $\rho = v$. Here, $G_F(\rho)$ is an operator, which represents the state space equation defined in (11) and the output equation for the measured signals:

$$y_F = G_F(\rho)\begin{bmatrix}\delta_f\\ u\\ f_a\end{bmatrix}, \quad G_F(\rho) = \begin{bmatrix}A_F(\rho) & B_F(\rho)\\ C_F & D_F\end{bmatrix}, \tag{14}$$

where $y_F = [a_y\ \dot{\phi}\ \phi]^{\mathrm{T}}$ is the measured output, which contains the lateral acceleration, the derivative of roll angle, and the roll angle itself. $u = [u_c\ \Delta F_b]^{\mathrm{T}}$ contains the control torque and the difference in brake forces. The signal f_a is the fault, which contains both the front and the rear actuator faults on the active anti-roll bars. The form of the FDI filter $F(\rho)$ is the following:

$$r = F(\rho)\begin{bmatrix}y_F\\ u\end{bmatrix}, \tag{15}$$

where r is the residual output, which is the estimation of fault f_a. The FDI filter uses both the measured output y_F and the control inputs u.

In order to identify the individual faults successfully, it is crucial to have good fault models. One way to describe fault models is to introduce frequency weights

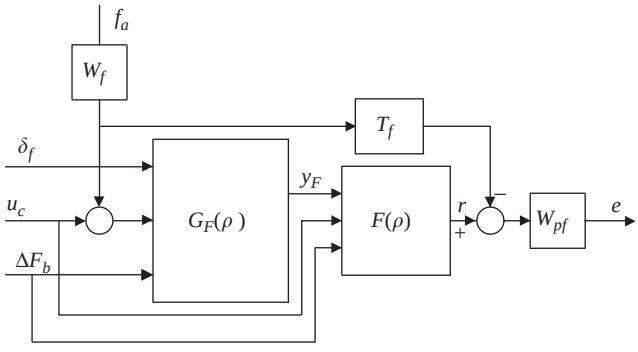

Fig. 2. Open-loop interconnection structure for FDI filter design.

on the fault signals, i.e. the fault f_a is modelled as a signal, which has flat power spectra and generates the frequency colored signal $W_f f_a$. In our case a constant diagonal weight is chosen in the whole frequency domain given by $W_f = 10$. The weight W_f means that the size of a possible fault is 10 kN m in the actuator channels. Then the filtered version of the fault can be considered. The filtered fault is given by $\bar{f} = T_f W_f f_a$, where T_f is the required transfer function from failure to the residual output. T_f is used to explicitly introduce time domain specification into the design process, i.e. to define the ideal tracking dynamics for the FDI filter. T_f is chosen for both types of failures to be $T_f = 1/(s+1)$.

W_{p_f} is the fault detection performance weight, which reflects the relative importance of the different frequency domains. The fault detection performance weight is a diagonal matrix with the following entries $W_{p_f} = 2[(s/3+1)/(s/0.1+1)]$. The weighting function W_{p_f} chosen for fault estimation errors can be considered as a penalty function, that is, the weight should be large in the frequency range in which small errors are desired and small in which larger errors can be tolerated. The size of the frequency response of weight W_{p_f} should be large at low frequency to achieve the integral action for fault estimation. Here, it is assumed that in the low frequency domain the fault estimation error should be rejected by a factor of 2 for both actuator failures. The fault estimation error is $e = W_{pf}(\bar{f} - r)$, where $\bar{f} = T_f W_f f$ and r is the residual output.

Applying the parameter-dependent yaw-roll dynamics $G_F(\rho)$ and the weighting functions in Fig. 2, the $\mathscr{H}_\infty$ filtering problem can be formulated (see Fig. 3) The augmented plant $P_F(\rho)$ in the filtering problem can be partitioned in the following form:

$$\begin{bmatrix} e \\ y_F \\ u \end{bmatrix} = \begin{bmatrix} P_{F11}(\rho) & P_{F12}(\rho) \\ P_{F21}(\rho) & P_{F22}(\rho) \end{bmatrix} \begin{bmatrix} w_F \\ r \end{bmatrix}, \tag{16}$$

where $w_F = [\delta_f \; u \; f_a]^{\mathrm{T}}$ and e is the fault estimation error. Using the FDI filter between u, y_F and r the closed-loop system $M_F(\rho)$ with respect to the FDI filter is given by a lower LFT structure:

$$M_F(\rho) = \mathscr{F}_\ell(P_F(\rho), F(\rho)) \tag{17}$$

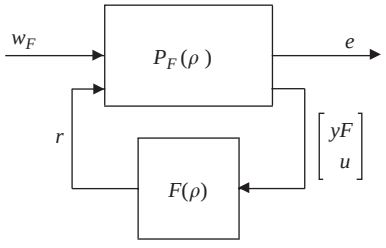

Fig. 3. Generalized model with the FDI filter.

in which the relationship between e and w_F is $e = M_F(\rho) w_F$.

The design requirement for the $\mathscr{H}_\infty$ residual generation is to maximize the effects of the fault on the residual and simultaneously minimize the effects of exogenous signals $(\delta_f, u_c, \Delta F_b)$ on the residual. To solve this problem, the optimization criterion can be formalized in the following form:

$$\inf_{F(\rho)} \sup_{\rho \in \mathscr{F}_{\mathscr{P}}} \sup_{\|w\|_2 \neq 0, w \in \mathscr{L}_2} \frac{\|e\|_2}{\|w_F\|_2}. \tag{18}$$

The optimization in Eq. (18) actually solves a fault estimation problem, in which e is the signal which is used to evaluate the estimation quality.

The performance index in Eq. (18) is the worst case distance between the fault estimation and itself the fault normalized by the size of the inputs. The operators from u to r, $M_{ru}(\rho)$, from δ_f to r, $M_{r\delta_f}(\rho)$ and from f_a to r, $M_{rf_a}(\rho)$ depend on the FDI filter $F(\rho)$. Minimizing the $\mathscr{H}_\infty$ norm of the $M_F(\rho)$ means that the operators $M_{ru}(\rho)$ and $M_{r\delta_f}(\rho)$ provide that the effect of exogenous signals is attenuated on the residual signal r. Moreover, $M_{rf_a}(\rho)$ keeps the fault sensitivity by minimizing the error to the fault.

The design of the FDI filter is based on the open-loop plant. In the nominal case the FDI filter design can be independently performed from the control design, i.e. independently from the compensator design (e.g. Niemann & Stoustrup, 1997a, b, 1998). It means that the FDI filter designed in open-loop system can be implemented in the closed-loop system.

Finally, the fault information provided by a fault detection filter is given by $\rho_f = \hat{f}/f_{max}$, where f_{max} is an estimation of the maximum value of the potential failure (fatal error). It means that the value of a possible fault is normalized into the interval [0 1]. More exactly, ρ_f, where r is the residual signal provided by the FDI filter and $r_{\max}$ is the maximum value of the potential failure (fatal error). The value 0 corresponds to the non-faulty operation and the value 1 means that the active anti-roll bars are not able to work. In case of 1 the only control input is the brake system. This fault information is used in the reconfiguration mechanism.

3.2. The reconfigurable control structure

In this section the setup of the reconfigurable control structure is presented for the fault tolerant roll stability system. Consider the closed-loop system in Fig. 4 which includes the feedback structure of the model $G_K(\rho)$ and the controller $K(\varrho)$, and elements associated with the uncertainty models and performance objectives. Here, $G_K(\rho)$, which is the basis of the control design, consists of the state equation defined in (11), the performance equation for the performance signals, and the output equation for the measured signals. The partitioned form

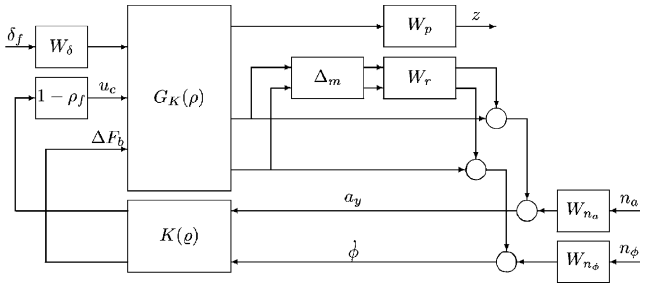

Fig. 4. The closed-loop interconnection structure for reconfigurable strategy.

of the $G_K(\rho)$ is the following:

$$\begin{bmatrix} z \\ y_K \end{bmatrix} = \begin{bmatrix} G_{K11}(\rho) & G_{K12}(\rho) \\ G_{K21}(\rho) & G_{K22}(\rho) \end{bmatrix} \begin{bmatrix} \delta_f \\ u \end{bmatrix}, \tag{19}$$

where $z = [z_a \; z_{F_z} \; u \; \Delta F_b]$ performance vector consists of the lateral acceleration, the lateral load transfers, the control inputs and the difference between the braking forces. $y_K = [a_y \; \dot{\phi}]$ is the measured output, which contains the lateral acceleration and the derivative of roll angle. $u = [u_c \; \Delta F_b]$ contains the control torques and the difference between the braking forces. The scheduling parameter of the $G_K(\rho)$ is the forward velocity: $\rho = v$. The form of the controller $K(\varrho)$ is the following:

$$u = K(\varrho) y_K. \tag{20}$$

The scheduling parameter ϱ in the controller structure consist of the ρ, which is same as used in the design of the FDI filter, and other parameters, which are defined later. In the figure n_a and n_ϕ represent the measurement noise associated with lateral acceleration and the derivative of the roll angle, respectively.

In the control design weighting functions are applied. The nominal model usually approximates the behavior of the plant well in the low-middle frequency domain, while in the high-frequency range the model differs from the plant. The uncertainties of the model are represented by W_r and Δ_m, where $\|\Delta_m\|_\infty < 1$. The weighting function W_r is selected $W_r = 2.25(S+20)/(S+450)$. The input weight W_δ normalizes the steering angle to the maximum expected command. The noise weight W_{n_a} for the lateral acceleration and W_{n_ϕ} for the derivative of roll angle $\dot{\phi}$ are chosen $0.01\,\mathrm{m/s^2}$ and 0.01 deg/s, respectively.

The purpose of the weighting functions is to keep the lateral acceleration, the lateral load transfers and the control inputs small over the desired frequency range. The weighting function W_{p_a} is selected to be parameter dependent:

$$W_{p_a} = \phi_a(R_r)\frac{(s/2000+1)}{(s/12+1)}, \tag{21}$$

where $\phi_a(R_r) = 2/(R_2 - R_1)(|R_r| - R_1)$ is a function of R_r. The parameter dependent gain $\phi_a(R_r)$ captures the relative importance of the acceleration response. When R_r is small, i.e., when the vehicle is not in an emergency, $\phi_a(R_r)$ is small, indicating that the LPV controller should not focus on minimizing acceleration, it should only generate a lateral displacement moment with the active anti-roll bars. On the other hand, when R_r has reached its critical value, that is $R_r = R_{crt}$, or the suspension has reached its physical limit, $\phi_a(R_r)$ is large, indicating that the controller should focus on preventing the rollover. Parameter R_1 defines the critical status when the rollover is imminent. Parameter R_2 shows how fast the controller should focus on minimizing the lateral acceleration. The weight $W_{p_{F_z}}$ is selected $\mathrm{diag}(1/10^2, 1/10^3)$, which means that the maximal gain of the lateral load transfers can be 10^2 for the front axle and 10^3 for the rear axle. The weight W_{p_u} is $\mathrm{diag}(1/20, 1/20)$, which corresponds to the front and rear control torques. The weight $W_{p_{F_b}}$ for the brake force is $1/10$.

On the event of a fault the range of the operation of the brake system must be extended and the wheels are decelerated gradually rather than rapidly if the normalized load transfer has reached its critical value. A small value of R_1 corresponds to activating the brake system early and gradually, whereas a large value of R_1 corresponds to activating the brake system rapidly. Thus, the design parameter R_1 is chosen to be scheduled on fault information ρ_f.

$$R_1 = R_1 - \frac{\rho_f}{10}, \tag{22}$$

where ρ_f is the normalized value of the fault information.

In order to describe the control objective, the parameter dependent augmented plant $P_K(\varrho)$ must be built up using the closed-loop interconnection structure in Fig. 4. The augmented plant $P_K(\varrho)$ includes the parameter dependent yaw-roll dynamics $G_K(\rho)$ and the weighting functions.

$$\begin{bmatrix} z \\ a_y \\ \dot{\phi} \end{bmatrix} = \begin{bmatrix} P_{K11}(\varrho) & P_{K12}(\varrho) \\ P_{K21}(\varrho) & P_{K22}(\varrho) \end{bmatrix} \begin{bmatrix} w_K \\ u \end{bmatrix}, \tag{23}$$

where $w_K = [\delta_f \; n_a \; n_\phi]$. In the LPV model of the yaw-roll motion three parameters are selected: the forward velocity v, the normalized lateral load transfer at the rear side R_r and the actuator fault information ρ_f, which is associated with the active anti-roll bars.

$$\varrho = [v \; R_r \; \rho_f], \tag{24}$$

where v is measured directly, ρ_f is provided by the FDI filter, while parameter R_r can be calculated by using the measured roll angle of the unsprung mass $\phi_{t,r}$.

Using the controller K between u and y_K the closed-loop system $M_K(\varrho)$ is given by a lower LFT structure:

$$M_K(\varrho) = \mathscr{F}_\ell(\mathscr{P}_K(\varrho), \mathscr{K}(\varrho)). \tag{25}$$

The control goal is to minimize the induced $\mathscr{L}_2$ norm of a LPV system $M_K(\varrho)$, with zero initial conditions, which is given by

$$\|M_K(\varrho)\|_\infty = \sup_{\varrho\in\mathscr{F}_\mathscr{P}} \sup_{\|w_K\|_2\neq 0, w_K\in\mathscr{L}_2} \frac{\|z\|_2}{\|w_K\|_2}. \tag{26}$$

In other words the goal is to design an LPV controller which minimizes the lateral acceleration and the lateral load transfers during a maneuver generated by the steering angle δ_f.

If $M_K(\varrho)$ is quadratic stable, this quantity is finite. The quadratic stability can be extended to the parameter dependent stability, which is the generalization of the quadratic stability concept. Applying the parameter dependent stability concept, it is assumed that the derivative of parameters can also be measured in real time. This concept is less conservative than the quadratic stability (Wu, 2001). The quadratic LPV γ-performance problem is to choose the parameter-varying controller in such a way that the resultant closed-loop system is quadratically stable and the induced $\mathscr{L}_2$ norm from w to z is less than γ. The existence of a controller that solves the quadratic LPV γ-performance problem can be expressed as the feasibility of a set of linear matrix inequalities (LMIs), which can be solved numerically. The state space representation of the augmented plant $P_K(\varrho)$ is formalized in the following way:

$$\begin{bmatrix} \dot{x} \\ z \\ y_K \end{bmatrix} = \begin{bmatrix} A(\varrho) & B_1(\varrho) & B_2(\varrho) \\ C_1(\varrho) & D_{11}(\varrho) & D_{12}(\varrho) \\ C_2(\varrho) & D_{21}(\varrho) & D_{22}(\varrho) \end{bmatrix} \begin{bmatrix} x \\ w_K \\ u \end{bmatrix}. \tag{27}$$

Theorem 2. *Given a compact set $\mathscr{P}\subset\mathscr{R}^S$, the performance level γ and the LPV system* (27)*, with restriction $D_{11}(\varrho)=0$, the parameter-dependent γ-performance problem is solvable if and only if there exist a continuously differentiable function $X:\mathscr{R}^S\to\mathscr{R}^{n\times n}$, and $Y:\mathscr{R}^S\to\mathscr{R}^{n\times n}$, such that for all $\varrho\in\mathscr{P}$, $X(\varrho)=X^{\mathrm{T}}(\varrho)>0$, $Y(\varrho)=Y^{\mathrm{T}}(\varrho)>0$ and*

$$\begin{bmatrix} \hat{A}(\varrho)X(\varrho)+X(\varrho)\hat{A}^{\mathrm{T}}(\varrho)-\sum_{i=1}^{s}\left(v_i\frac{\partial X}{\partial\varrho_i}\right)-B_2(\varrho)B_2^{\mathrm{T}}(\varrho) & X(\varrho)C_1^{\mathrm{T}}(\varrho) & \gamma^{-1}B_1(\varrho) \\ C_1(\varrho)X(\varrho) & -I_{n_e} & 0 \\ \gamma^{-1}B_1^{\mathrm{T}}(\varrho) & 0 & -I_{n_d} \end{bmatrix} < 0, \tag{28}$$

$$\begin{bmatrix} \tilde{A}^{\mathrm{T}}(\varrho)Y(\varrho)+Y(\varrho)\tilde{A}(\varrho)+\sum_{i=1}^{s}\left(v_i\frac{\partial Y}{\partial\varrho_i}\right)-C_2^{\mathrm{T}}(\varrho)C_2(\varrho) & Y(\varrho)B_1(\varrho) & \gamma^{-1}C_1^{\mathrm{T}}(\varrho) \\ B_1^{\mathrm{T}}(\varrho)Y(\varrho) & -I_{n_d} & 0 \\ \gamma^{-1}C_1(\varrho) & 0 & -I_{n_e} \end{bmatrix} < 0, \tag{29}$$

$$\begin{bmatrix} x(\varrho) & \gamma^{-1}I_n \\ \gamma^{-1}I_n & Y(\varrho) \end{bmatrix} \geqslant 0, \tag{30}$$

where $\hat{A}(\varrho)=A(\varrho)-B_2(\varrho)C_1(\varrho)$, $\tilde{A}(\varrho)=A(\varrho)-B_1(\varrho)C_2(\varrho)$.

The state space representation of the LPV control $K(\varrho)$ is constructed from the solutions $X(\varrho)$ and $Y(\varrho)$ of the LMI optimization problem. The Theorem 2 and its proof are found in Wu (1995, 2001).

The constraints set by the LMIs in Theorem 2 are infinite dimensional, as is the solution space. The variables are $X, Y:\mathscr{R}^S\to\mathscr{R}^{n\times n}$, which restricts the search to the span of a collection of known scalar basis functions. Select scalar continuous differentiable basis functions $\{g_i:\mathscr{R}^S\to\mathscr{R}\}_{i=1}^{N_x}$, $\{f_j:\mathscr{R}^S\to\mathscr{R}\}_{j=1}^{N_y}$, then the variables in Theorem 2 can be parameterized as $X(\varrho)=\sum_{i=1}^{N_x} g_i(\varrho)X_i$, $Y(\varrho)=\sum_{j=1}^{N_y} f_j(\varrho)Y_j$. Currently, there is no analytical method to select the basis functions, namely g_i and f_i. An intuitive rule for basis function selection is to use those present in the open-loop state space data. In our case, several power series $\{1,\varrho^2\}$ of the scheduling parameters are chosen based on the lowest closed-loop $\mathscr{L}_2$ norm achieved.

The infinite-dimensionality of the constraints is relieved by approximating the parameter set $\mathscr{P}$ by a finite, sufficiently fine grid $\mathscr{P}_{grid}\subset\mathscr{P}$. For the interconnection structure, $\mathscr{H}_\infty$ controllers are synthesized for several values of velocity in a range $v=[40\,\text{kmph},\ldots,100\,\text{kmph}]$. The spacing of the grid points is based upon how well the $\mathscr{H}_\infty$ point designs perform for plants around the design point. Seven grid points are selected for the velocity scheduling parameter design space.

The rear load transfer parameter space is grided as $R_r=[0,\ R_1,\ R_2,\ 1]$. The scheduling parameter ρ_f, which is the fault information provided by the FDI filter, can be taken from interval $\rho_f=[0,\ 1]$. The zero value of ρ_f corresponds to the non-faulty operation and the value 1 to the full hydraulic actuator failure. Hence the parameter ρ_f is grided as $\rho_f=[0,\ldots,1]$ by selecting five grid points. Weighting functions for both the performance and robustness specifications are defined in all of the grid points. With respect to the robustness requirement, the same frequency weighting functions are applied in the whole parameter space and the effect of the scheduling parameter is neglected. It is a reasonable engineering assumption, since uncertainties (i.e. unmodelled dynamics, parametric uncertainties) do not depend on forward velocity and other scheduling parameters. The implementation of the reconfigurable control structure is shown in Fig. 5.

4. Demonstration examples

In this section, illustrative examples are shown for the roll control mechanism, which is based on the reconfigurable LPV control. In the first simulation example, a

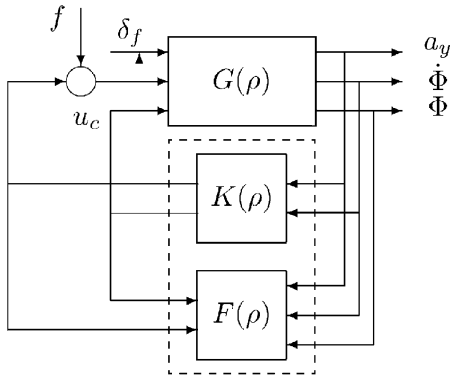

Fig. 5. The implementation of the reconfigurable control structure.

double-lane change maneuver is performed. This maneuver is often used to avoid an obstacle in an emergency. The maneuver has 2.5 m path deviation over 100 m. The size of the path deviation is chosen to test a real obstacle avoidance in an emergency on road. The velocity of the vehicle is 70 kmph. The steering angle input is generated in such a way that the vehicle with no roll control would come close to a rollover during the maneuver and its normalized load transfers would be over ± 1. Recall that the yaw-roll model is only valid if the normalized load transfers are below the value ± 1 for both axles. In order to avoid an unrealistic change in the steering angle, a ramp signal is applied at which the signal reaches the

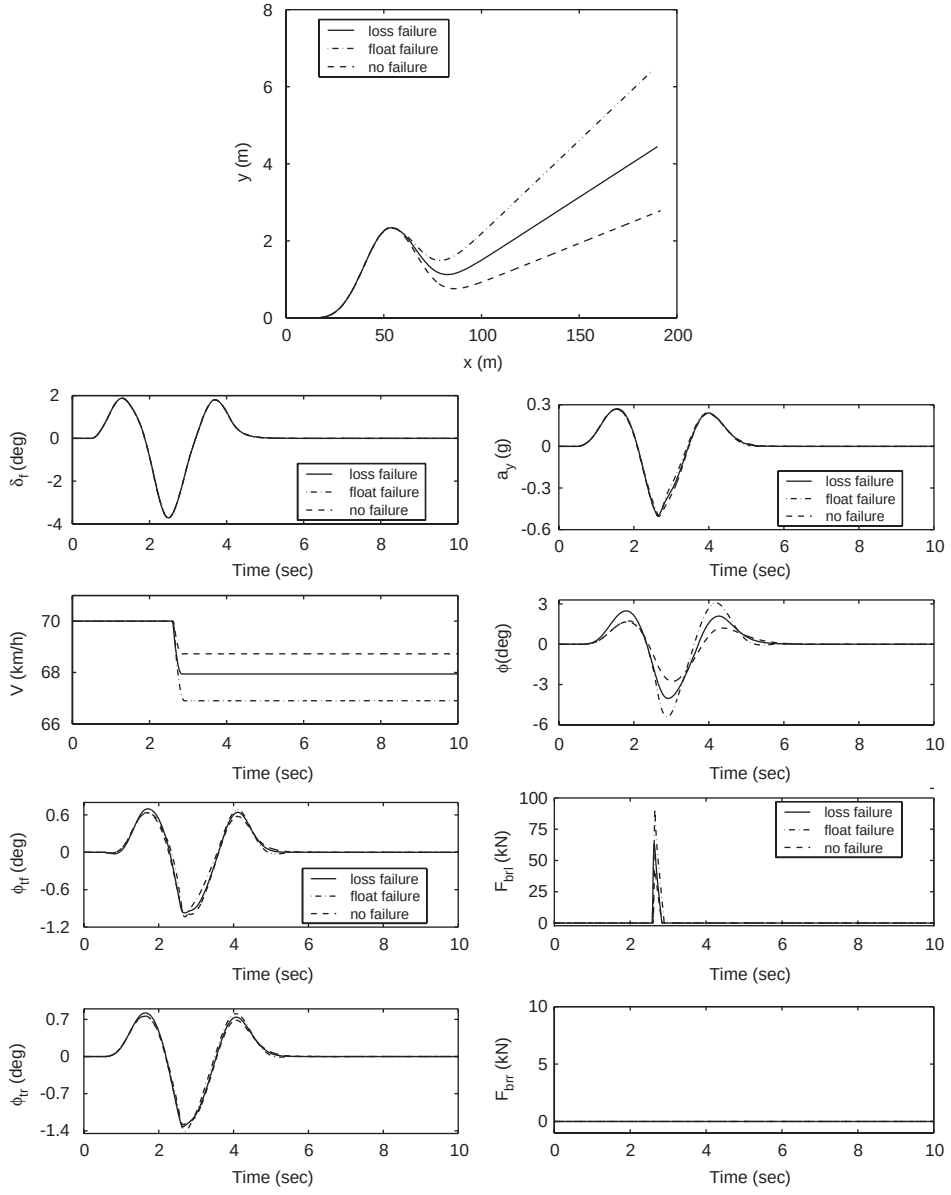

Fig. 6. Time responses to double-lane change steering input in different failure situations.

maximum value (3.5°) in 0.5 s and filtered at 4 rad/s to represent the finite bandwidth of the driver. During this maneuver an actuator failure is used in the simulation so that the reconfiguration properties of the controller can be analyzed.

In practice, three fault scenarios can be considered for a hydraulic actuator. First is a lock failure, in which case the piston of hydraulic actuator remains locked in a particular position. In this case, the hydraulic actuator does not work after the fault and the actuator resists the motion of vehicle in the roll plane. The physical characteristic of this phenomenon is that the piston of hydraulic actuator is clutched and it is not moving any longer. Second is a floating failure, in which case the relative displacement of the hydraulic actuator changes the suspension travel instantaneously. This means that the active anti-roll bars cannot generate lateral displacement moment to balance the overturning moment and the piston of hydraulic actuator can move freely in the cylinder. This situation may arise when the power supply is cut off and sufficient oil pressure is not provided. The third type of failure is the loss in effectiveness. This means that actuator effectiveness is reduced. When this failure occurs the actuator goes on working even with reduced power. This is the case for example when the leakage coefficient of the piston is too high, hence the actuator cannot generate the torque required by the control valve. In the yaw-roll model all actuator faults are handled by additive structures.

In our case, the ρ_f normalized scheduling parameter is used to adjust the controller with different types of actuator failures. When the ρ_f is equal to 1, this situation can be classified as a float failure because the anti-roll bars have broke down but the hydraulic actuators do not resist the displacement of the suspension. In this case the only control input which can prevent the rollover of vehicle is the brake system. If ρ_f takes the value between 0 and 1 there is a loss in effectiveness. That is, the active anti-roll bars can be used even with reduced power to generate stabilizing moment.

In the first simulation the ρ_f is set at the constant value 0.7. In this case actuator effectiveness is reduced by 70%. The second fault scenario is when the ρ_f is a ramp signal with unity slope starting from 1.5 to 2.5 s. Here, the fault is that actuator effectiveness decreases gradually to zero. Using different fault scenarios the responses of yaw roll dynamics are compared. Figs. 6 and 7 show the responses in case of a float-type failure (dash-dot), loss in effectiveness failure (solid) and the non faulty situation (dash) respectively.

The lateral acceleration in all cases is slightly different. The reason for this fact is that where the normalized load transfers do not reach the critical value

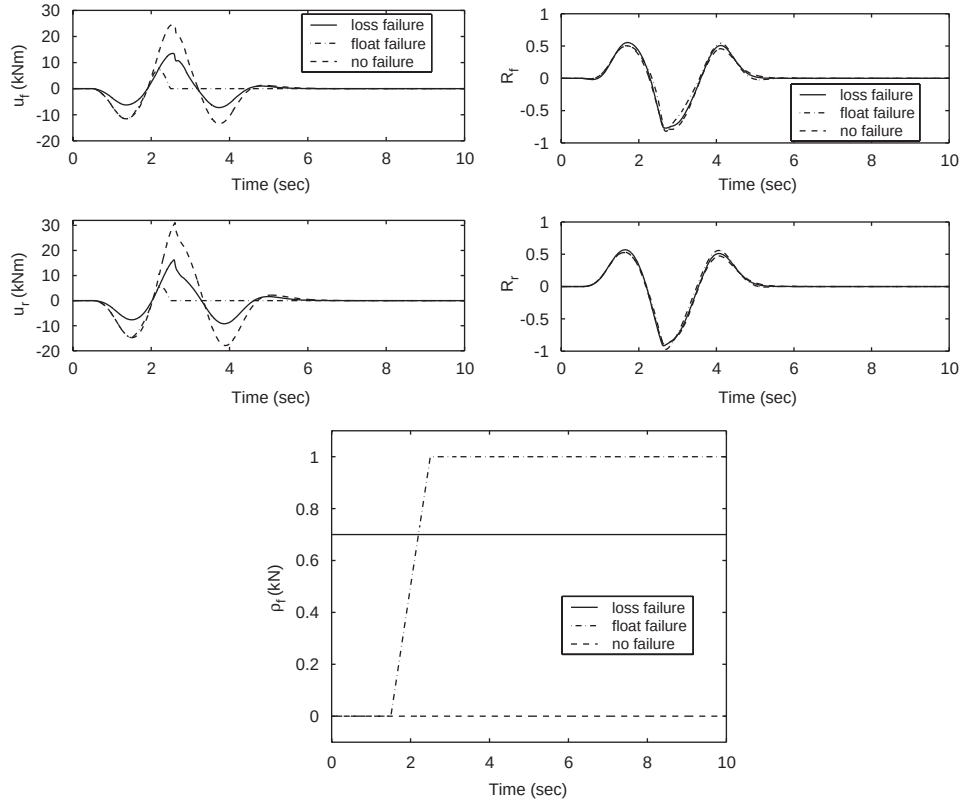

Fig. 7. Time responses to double-lane change steering input in different failure situations (Continued).

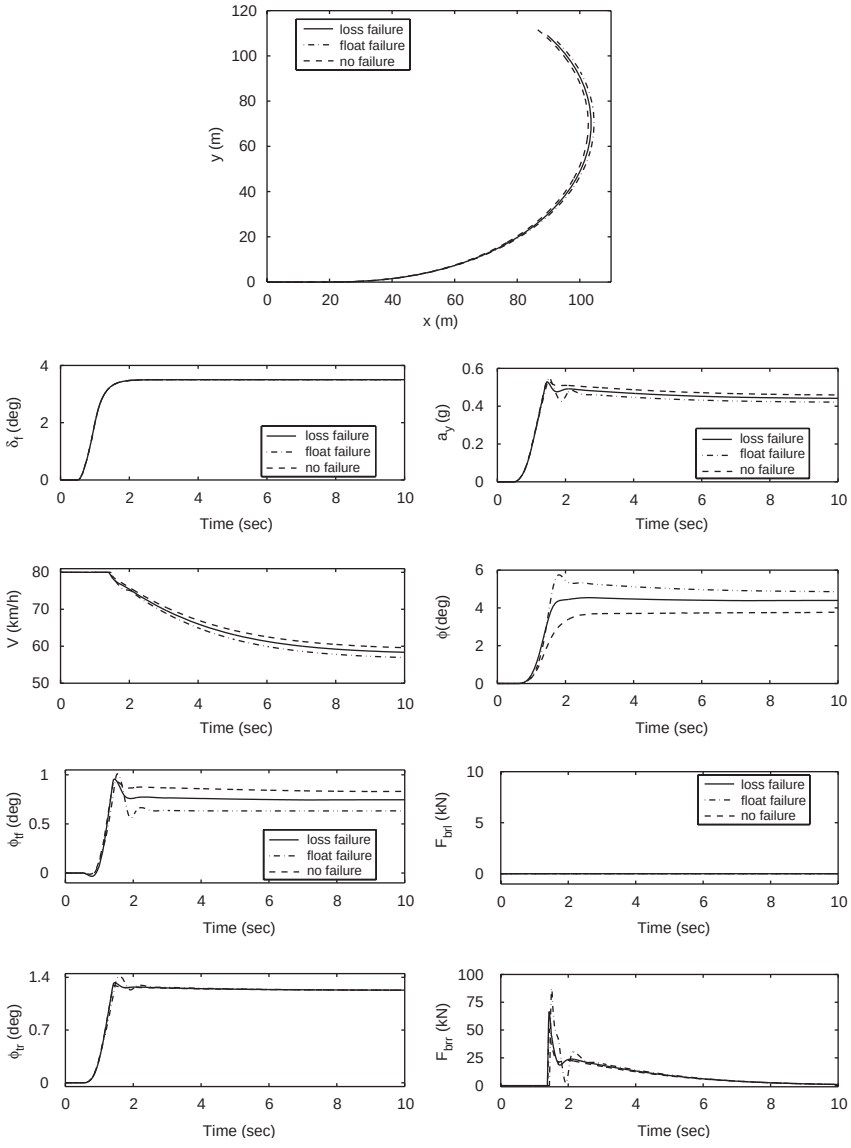

Fig. 8. Time responses to cornering in different failure situations.

R_1 only the active anti-roll bars are activated and the brake system is not used. However the active anti-roll bars are not able to decrease lateral acceleration because they do not have a direct effect on changing acceleration. So the effect of a fault in the actuator does not appear in lateral acceleration. It can be observed that, when faults occur, the roll angle increases due to the reduced power of the hydraulic actuators. In the absence of a fault the actuator can generate higher control torque than when a fault is present, so it can balance the primary overturning moment more effectively. The roll angles of the unsprung masses for front and rear axles are slightly different due to the different suspension parameters and the stiffness to load ratio. Note, that the relative roll angle of the suspension $(\phi - \phi_{t,i})$ is within the acceptable limit, which is about 7–8°. It can be seen that the control torque is smaller in the case of loss failure than in a fault-free situation. In the case of float-type failure its effectiveness decreases gradually and it becomes zero when the normalized fault information has reached value 1.

The required brake force is the largest in the case of a float failure. This is because the active anti-roll bars are not able to generate control torque over 2.5 s, so the reconfigured controller structure is identical to the controller in which only the brake system is used to prevent the rollover of the vehicle. In the fault-free case the active anti-roll system is working and generates stabilizing lateral displacement moment. Hence, the brake force required to prevent the rollover of the vehicle is less than in the faulty cases. The paths of the vehicle corresponding to each case can also be seen in the figure. In the case of the lock failure the real path is much different from the desired path due to the

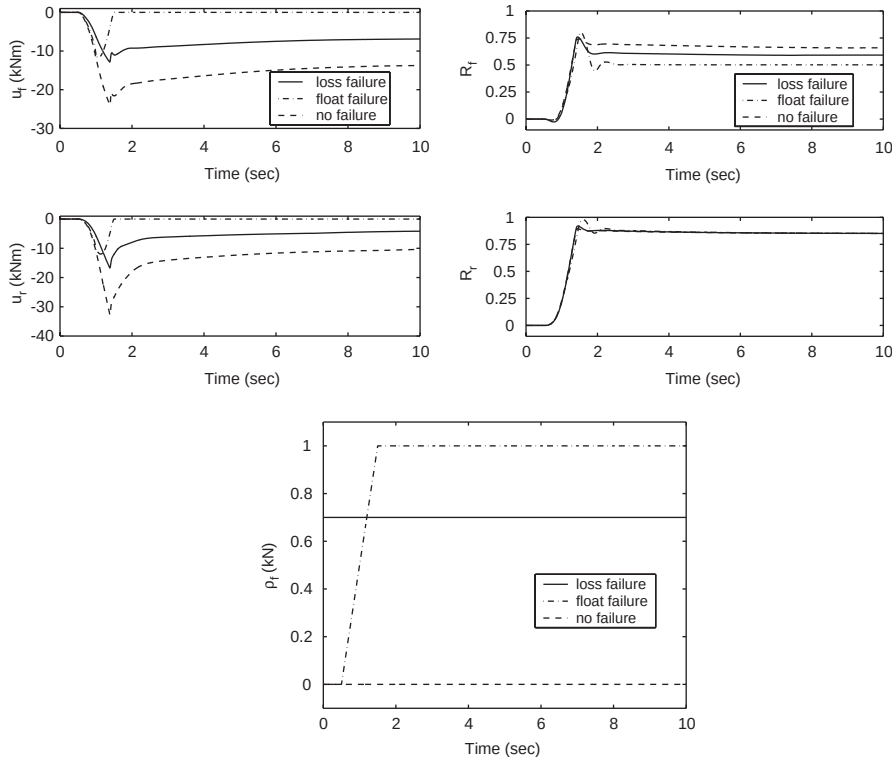

Fig. 9. Time responses to cornering in different failure situations (Continued).

increased brake moment which affects the yaw motion. In the case of a fault-free situation the deviation of the real and the desired path is smaller than in the faulty cases.

In the next example, the cornering responses of a single unit vehicle model travelling at 90 kmph can be seen. In the case of a loss failure the ρ_f is set at the constant value 0.7, and in the case of a float-type failure the ramp signal starts from 0.5 s and reaches the value 1 in 1.5 s. Figs. 8 and 9 show the responses to the float-type failure (dash-dot), the loss in effectiveness failure (solid) and the non-faulty situation (dash), respectively. The steering angle applied in the simulation is a step signal. It can be observed that in the faulty cases the roll angle increases due to the reduced power of the hydraulic actuators. The relative roll angle stays within the acceptable limit in each case. However, it can be seen that the relative roll angle of the suspension has reached the acceptable limit because of the reduced control torque, when the actuator fails. The roll angle of the unsprung masses is slightly different due to the different suspension parameters and the stiffness to load ratio.

As the lateral acceleration increases, the normalized load transfer increases more quickly at the rear axle than at the front axle since the ratio of the effective roll stiffness to the axle load is larger at the driven axle. The normalized load transfers do not exceed the value ± 1 in any of the cases, which means that the lateral force on one of the curve inner side wheels will not become zero. In the cornering maneuver the active anti-roll control is not sufficient to prevent the rollover of the vehicle. Consequently, the normalized load transfers reach the critical value R_1 during the cornering maneuver so the brake control is activated and the brake system reduces the lateral acceleration. The time when the brake control is activated can be seen in the brake force figure, which shows that the rear right-hand side wheel is braked to prevent the rollover of the vehicle. The largest brake force is required in the case of float-type failure because the actuator fails totally after 1.5 s. The control torque is larger in the faulty cases than in non-faulty situation.

5. Conclusion

This paper has developed a reconfigurable control structure. This structure combines an active anti-roll bar control with an active brake control and applies an FDI filter, which identifies the different actuator failures. The control design is based on the LPV modelling, in which the forward velocity, the normalized lateral load transfer and the residual output of the FDI filter are chosen as scheduling parameters. The design of the FDI filter is based on the LPV model of the vehicle, in which the scheduling parameter is the forward velocity of the vehicle. The control design and the FDI design are performed independently from each other. That is the reason why the scheduling parameter applied in the FDI

design differs from the scheduling parameters applied in the control design. The reconfigurable control is guaranteed in such a way that the control design uses the residual signal as an input which is generated by the FDI filter.

References

Abdalla, M. O., Nobrega, E. G., & Grigoriadis, K. M. (2001). Fault detection and isolation filter design for linear parameter varying systems. In *Proceedings of the American control conference* Arlington (pp. 3890–3895).

Abe, M. (1994). A study on effects of roll moment distribution control in active suspension on improvement of limit performance of vehicle handling. *International Journal of Vehicle Design*, *15*, 326–336.

Ackermann, J., & Odenthal, D. (1999). Damping of vehicle roll dynamics by gain scheduled active steering. In *Proceedings of the European control conference*.

Ackermann, J., Odenthal, D., & Bunte, T. (1999). Advantages of active steering for vehicle dynamics control. In *Proceedings of the international symposium on automotive technology and automation*. Vienna.

Becker, G., & Packard, A. (1994). Robust performance of linear parametrically varying systems using parametrically-dependent linear feedback. *System Control Letters*, *23*, 205–215.

Bokor, J., & Balas, G. (2004). Detection filter design for LPV systems—a geometric approach. *Automatica*, *40*, 511–518.

Chen, B., & Peng, H. (2001). Differential-braking-based rollover prevention for sport utility vehicles with human-in-the-loop evaluations. *Vehicle System Dynamics*, *36*(4–5), 359–389.

Chen, J., & Patton, R. J. (1999). *Robust model based fault diagnosis for dynamic systems*. Boston/Dordrecht/London: Kluwer.

Edelmayer, A., Bokor, J., Szigeti, F., & Keviczky, L. (1997). Robust detection filter design in the presence of time-varying system perturbations. *Automatica*, *33*(3), 471–475.

Frank, P., Palkovics, L., & Gianone, P. (2000). Using wheel speed and wheel slip information for controlling vehicle chassis systems. In *Proceedings of the fifth international symposium on advanced vehicle control*. Ann Arbor: USA.

Ganguli, S., Marcos, A., Balas, G. J., & Bokor, J. (2002). Reconfigurable LPV control design for B-747-100/200 longitudinal axis. In *Proceedings of the American control conference*. (pp. 3612–3617).

Gertler, J. (1997). Fault detection and isolation using parity relations. *Control Engineering Practice*, *5*(5), 653–661.

Hammouri, H., Kinnaert, M., & Yaagoubi, E. (1999). Observer-based approach to fault detection and isolation for nonlinear systems. *IEEE Transactions on Automatic Control*, *44*(10), 1879–1884.

Isermann, R. (2001). Diagnosis methods for electronic controlled vehicles. *Vehicle System Dynamics*, *36*, 77–117.

Isermann, R., Schwarz, R., & Stolz, S. (2002). Fault-tolerant drive-by-wire systems. *IEEE Control Systems Magazine*, 64–81.

Jeppesen, B. P., & Cebon, D. (2001). Real-time fault identification in an active roll control system. In *17th IAVSD symposium*. Coppenhagen.

Kanev, S., & Verhaegen, M. (2000). Controller reconfiguration for non-linear systems. *Control Engineering Practice*, *8*, 1223–1235.

Leith, D. J., & Leithead, W. E. (2000). Survey of gain-scheduling analysis and design. *International Journal of Control*, *73*(11), 1001–1025.

Lin, R. C., Cebon, D., & Cole, D. J. (1996). Optimal roll control of a single-unit lorry. *Proceedings of the Institution of Mechnical Engineers, Journal of Automobile Engineering*, *210*, 44–55.

Massoumnia, M. A. (1986). A geometric approach to the synthesis of failure detection filters. *IEEE Transactions on Automatic Control*, *AC-31*(9), 839–846.

Niemann, H., & Stoustrup, J. (1997a). Integration of control and fault detection: Nominal and robust design. In *Proceedings of IFAC symposium on fault detection*. Hull. (pp. 341–346).

Niemann, H., & Stoustrup, J. (1997b). Robust fault detection in open loop vs. closed loop. In *Proceedings of the IEEE conference on decision and control*. San Diego. (pp. 4496–4497).

Odenthal, D., Bunte, T., & Ackermann, J. (1999). Nonlinear steering and braking control for vehicle rollover avoidance. In *Proceedings of the European control conference*.

Palkovics, L., Semsey, A., & Gerum, E. (1999). Roll-over prevention system for commercial vehicles—additional sensorless function of the electronic brake system. *Vehicle System Dynamics*, *32*, 285–297.

Persis, C., & Isidori, A. (2001). A geometric approach to nonlinear fault detection and isolation. *IEEE Transaction on Automatic Control*, *46*, 853–865.

Rough, W. J., & Shamma, J. S. (2000). Research on gain scheduling. *Automatica*, *36*, 1401–1425.

Sampson, D. J. M., & Cebon, D. (1998). An investigation of roll control system design for articulated heavy vehicles. In *Proceedings of the fourth international symposium on advanced vehicle control*. Nagoya: Japan. (pp. 311–316).

Sampson, D. J. M., & Cebon, D. (2003). Active roll control of single unit heavy road vehicles. *Vehicle System Dynamics*, *40*, 229–270.

Stoustrup, J., & Niemannn, H. (1998). Fault detection for nonlinear systems—a standard problem approach. In *IEEE conference on decision and control*. Tampa. (pp. 96–101).

Szabo, Z., Bokor, J., & Balas, G. (2002). Detection filter design for lpv systems—a geometric approach. In *Proceedings of the IFAC world congress*. Barcelona.

Szaszi, I., Marcos, A., Balas, G. J., & Bokor, J. (2001). LPV detection filter design for a Boeing 747-100/200 aircraft. In *Proceedings of the AIAA guidance, navigation and control conference*. (pp. 4957).

Szigeti, F., Vera, C. E., Bokor, J., & Edelmayer, A. (2001). Inversion based fault detection and isolation. In *40th IEEE conference on decision and control*. (pp. 1005–1010).

Wu, F. (1995). *Control of linear parameter varying systems*. Ph.D. thesis, University of California at Berkeley.

Wu, F. (2001). A generalized LPV system analysis and control synthesis framwework. *International Journal of Control*, *74*, 745–759.